DOE/PC/90291--T10

DOE/PC/90291--T10

DE93 008103

DESIGN OF A HIGH ACTIVITY AND SELECTIVITY ALCOHOL CATALYST

Ninth Quarterly Report for Period
August 7, 1992 to November 7, 1992

Henry C. Foley and G. Alex Mills
Coprincipal Investigators

Center for Catalytic Science and Technology
Department of Chemical Engineering
University of Delaware
Newark, Delaware 19716

Date Published:
November 30, 1992

Prepared for
Fossil Energy
Department of Energy

Under Award No. DE-FG22-90PC 90291

US/DOE Patent Clearance is not required prior to publication of this document.

Executive Summary

The focus of this update concerns our efforts to synthesize bimetallic cluster-derived Rh-Mo catalysts for CO and CO_2 hydrogenation to preferentially produce oxygenates. The rhodium-molybdenum cluster, $(PPh_3)_2RhMo(CO)(\mu\text{-}CO)_2Cp$, has been employed as a precursor to alumina- and silica-supported catalysts; these catalysts have been applied in the hydrogenation of carbon monoxide. When compared to catalysts made from the distinct organometallic complexes, $RhH(CO)(PPh_3)_3$ and $[Mo(CO)_3Cp]_2$, the catalysts derived from a binuclear precursor show significantly higher activities for CO hydrogenation and superior selectivities towards oxygenates, namely, methanol, dimethyl ether and ethanol. Product distributions of the oxygenates greatly depend on the type of support. Fourier transform infrared spectroscopy studies indicated that CO chemisorbs on the cluster-derived catalysts mainly as gem-dicarbonyls while it is chemisorbed only in the linear-carbonyl configuration on the catalysts made from separate rhodium and molybdenum complexes. When considered in the light of the close proximity of the Rh and Mo atoms in the binuclear precursor, this gem-dicarbonyl feature of the CO adsorption on the cluster-derived catalysts may imply an electron density transfer from Rh towards Mo during reduction and/or reaction. The particular oxygenate selectivity of the cluster-derived catalysts may be correlated to the strong electronic interaction between Rh and Mo. Carbon dioxide hydrogenation has also been carried out on the catalysts mentioned above. Again, the cluster-derived catalysts show higher oxygenate selectivities than others examined in the study. Finally, the catalysts were studied with regard to both CO and CO_2 hydrogenation kinetics. Apparent activation energies have been inferred based on changes in activities of corresponding reactions with changes in reaction temperature.

Introduction

Recent investigations in the catalytic chemistry literature have focused on promoted rhodium catalysts with particular emphasis on the promotional effects of molybdenum and on organometallic-derived Rh-Mo catalysts[1-12]. H. Miessner and M. Ichikawa et al.[1-4] have published investigations of bimetallic cluster-derived Rh-Mo catalysts. These cluster-derived catalysts have shown significant oxygenate selectivity in CO hydrogenation when compared with bimetallic catalysts made from metal salts. There are various explanations for the strong promotional effects of the molybdenum on supported rhodium catalysts. Most such explanations tend to attribute the effects to coverage of large rhodium particles by a molybdenum suboxide or to the formation of mixed oxides of rhodium and molybdenum which are thought to be responsible for improved oxygenate selectivity[1,5,6]. This kind of reasoning is probably true when applied to catalysts made from separate metal salts as initial materials and with high metal loadings because of the aggregation of the metals during reduction. But this explanation can not account for the result that Rh-Mo bimetallic cluster-derived catalysts have even higher oxygenates selectivity than conventional bimetallic catalysts. The high oxygenate selectivity of such cluster-derived catalysts implies that intrinsic metal-metal interactions present in the catalyst precursor indeed result in different promoting behavior, as reported by Miessner and Ichicawa et al[1-4] as well as this paper. In their most recent paper[8], Miessner et al. also excluded molybdenum suboxide migration; instead they explained that the Mo promotion results in oxidative disruption of Rh_X particles and prevents the sintering of Rh. By reducing Rh sintering, the catalyst retains a high number of active sites on the boundary of small Rh particles even for the catalysts derived from separate complexes. Based on our investigation of cluster derived Rh-Mo bimetallic catalysts, particularly with regard to our infrared spectroscopic results, it seems reasonable to attribute the promotion of rhodium by molybdenum to a more direct electronic

interactions between rhodium and molybdenum, stemming, perhaps, from the presence of such an interaction in the binuclear precursor.

Experimental

The bimetallic cluster, $(PPh_3)_2RhMo(CO)(\mu\text{-}CO)_2Cp$, was synthesized following the method reported by Preston et al[9]. Initial complexes, $RhCl(PPh_3)_3$, $Mo(CO)_6$, NaCp/THF, $RhH(CO)(PPh_3)_3$ and $[Mo(CO)_3Cp]_2$ were purchased from Strem and Aldrich and were used without further purification. Gamma-alumina (American Cyanamid, BET surface area= 250 m^2/g) and Silica (BET surface area=?m^2/g) were heated at 200°C in air for 24 hours before catalyst preparation.

The impregnation method was employed for catalyst preparation. Calculated amounts of cluster or separate complexes were dissolved in dichloromethane and the solution was added to corresponding amounts of support under a N_2 atmosphere. The mixture was then stirred for 2 hours and finally the solvent was removed by vacuum evaporation. The calculated rhodium loading for all the samples presented in this study was 0.5%wt and the samples have a mole ratio of Rh to Mo of 1.

CO or CO_2 hydrogenation activities of the catalysts were tested in a fixed-bed high pressure reactor. Detailed descriptions of the reactor system, product analysis and pretreatment of gases can be seen in elsewhere[10]. The reactor was charged with 1.0g of catalyst (approximately 60x100 mesh). The catalyst was oxidized at 200°C in flowing air (30 ml/min) for 4 hours and then reduced at 350°C for 6 hours in flowing H_2 (40ml/min). After the catalyst reached its stable activity, reaction data were collected at different reaction conditions: 200 to 350°C; 1.0MPa to 3.0MPa; CO/H_2 or CO_2/H_2=2 to 0.33; GHSV= 1200 to 2400h^{-1}.

Reaction rate is expressed as follows:

$$r = \frac{X \cdot F}{(22414 \cdot 60 \cdot W)} \qquad \text{(mole of CO or } CO_2\text{/gRh/Sec.)}$$

where, X is the conversion of CO or CO_2; F is flow rate of CO or CO_2 (ml/min) at NTP; W is weight (g) of Rh in sample.

The selectivity (S_i) toward product *i* is defined as:

$$S_i = (n_i \cdot C_i)/(\Sigma n_i \cdot C_i)$$

where n_i is the carbon number of the product *i* and C_i is the mole percentage of the component *i* detected.

Based on reaction rate and selectivity data and their respective temperature dependence, the natural log of the rate was plotted versus inverse temperature and activation energies for the total reaction and each product formed were calculated from the slop of the fitted line. To determine the reaction orders for total reaction and each product formed (total conversion of CO or CO_2 was maintained at less than 7%) with respect to partial pressure of H_2 and CO (or CO_2), the total reaction rate and formation rate of each product were measured while varying the partial pressure of both H_2 and CO (or CO_2) and these data were fitted by using least-square regression with *Mathematica* to a linearized general power law for the rate as follow:

$$\ln(r) = \ln(k) + x \cdot \ln(PH_2) + y \cdot \ln(PCO \text{ or } PCO_2)$$

where k, x and y are rate constant, rate order with respect to partial pressure of H_2 and CO (or CO_2), respectively.

In situ infrared spectroscopic studies of the catalysts were performed on a Nicolet 510 FT-IR spectrometer using a self-supported sample wafer in an *in situ* IR cell. All spectra were recorded at 50 scans with a resolution of 4 cm^{-1}. The mounted wafer was

treated in a similar way to the pretreatment of catalyst sample in the reaction tests and then the cell was evacuated at 10^{-3} torr. 50 torr of CO was introduced to the wafer at room temperature. IR spectra were recorded while evacuating the IR cell at different temperatures.

Result and Discussion

Since Fischer and Tropsch[13,14] reported that CO could be catalytically hydrogenated to a broad range of organic compounds in 1926, great efforts have been invested to develop a selective catalytic system to break down the so-called Anderson-Schulz-Flory distribution of the products. With more public attention focused on the reduction of petroleum dependence and on protecting the environment by producing synthetic components for gasoline blends, interest in CO hydrogenation to oxygenates by promoted rhodium catalysts has greatly increased. In contrast to traditional salt-derived bimetallic catalysts, bimetallic cluster-derived catalysts have several advantages: structural characteristics, adjustable metal skeletons, number and/or type of ligands, etc. The continued development of organometallic chemistry offers great opportunities and possibilities in this regard.

The positive promotional effect of Mo on supported Rh catalysts for CO hydrogenation motivated us to develop a Rh-Mo cluster-derived catalysts which also includes phosphorous as a possible acidic promoter and/or selective inhibitor. In fact, the supported $(PPh_3)_2RhMo(CO)(\mu\text{-}CO)_2Cp$ derived Rh-Mo catalysts indeed behave differently from other catalysts when tested in CO or CO_2 hydrogenation.

1. *CO Hydrogenation Activity and Selectivity*

The CO hydrogenation reaction conditions and results are summarized in Table 1. The results indicated that compared with the catalysts, $Rh,Mo/SiO_2$ and $Rh,Mo/Al_2O_3$, derived from the mononuclear complexes, bimetallic cluster-derived catalysts show

higher activities for CO hydrogenation. In addition, the alumina-supported bimetallic cluster shows particularly high activity. With regard to total oxygenate selectivity, cluster-derived catalysts have a superior product yield. Beyond the differences correlated to the active metal phase, different supports seem to alter oxygenate distribution: methanol is the main oxygenate on silica-supported catalysts while a much higher percentage of dimethyl ether is formed on the alumina-supported catalysts compared to other oxygenates. We believe, methanol is dehydrated to dimethyl ether (i.e. dimethyl ether is a secondary product) on alumina-supported catalysts because of the significant Lewis acidity of the alumina surface.

2. *CO_2 Hydrogenation Activity and Selectivity*

Table 2 summarizes the reaction conditions and results for CO_2 hydrogenation testing of the catalysts. It can be seen that the activity of the catalysts for CO_2 hydrogenation is lower than that of CO hydrogenation, but again, the cluster-derived catalysts show distinctly higher selectivities toward oxygenates compared with catalysts derived from separate complexes. The differences in the product distributions from those of CO hydrogenation are that methanol is the main oxygenated component for both kinds of oxide-supported catalysts. Nevertheless, dimethyl ether was once again formed on the alumina-supported catalysts. As mentioned above, dimethyl ether is formed by secondary dehydration of methanol formed from CO and that the acidity of the catalysts dominate the dehydration. Therefore, the different dimethyl ether selectivity of CO and CO_2 hydrogenation on the same catalyst should originate from the different basicity of CO and CO_2, i. e. the weak Lewis basicity of CO_2[15] may block some of the Lewis acid sites. Another possible reason for the difference in the dimethyl ether formation is related to the reverse water-gas shift reaction. When a mixture of CO_2 and H_2 is feed to the reactor, the CO_2 can undergo reverse water-gas shift and produce both CO and H_2O. Water formed in this transformation could dissociatively adsorb on the Lewis acid sites of

the support surface, and inhibit the dehydration of methanol. In contrast, when CO is fed to the reactor, the water-gas shift equilibrium is driven forward, consuming water which might otherwise inhibit dehydration of methanol.

3. *The Effect of Reaction Conditions on Selectivity*

Temperature can dramatically change the selectivity of CO and CO_2 hydrogenation on both cluster-derived and mononuclear complex-derived catalysts. Although the changes are similar, the cluster-derived catalysts show much more activity and selectivity to oxygenates at lower temperatures compared with the corresponding mononuclear complex-derived catalysts. Figure 1 and 2 demonstrate this superior performance of the cluster-derived Rh-Mo catalyst by depicting the product selectivity as a function of temperature. Methanol selectivity, for example, is approximately twice as high (80% compared to 45%) at 250°C over the $RhMo/SiO_2$ than over the $Rh,Mo/SiO_2$.

The reaction rate and oxygenate selectivity increase, and hydrocarbon selectivity decreases, with increasing total pressure. The CO/H_2 or CO_2/H_2 ratio can effect the selectivity of oxygenates though this effect is not as strong as the effect of varying temperature. With higher hydrogen partial pressure, higher oxygenate selectivity can be realized. (Fig. 3).

Finally, Figure 4 demonstrates that the cluster-derived catalysts are very stable after break-in. In Figure 4, CO hydrogenation rate and methanol selectivity of the reaction for $RhMo/SiO_2$ are seen to remain stable for nearly 100 hours on stream.

4. *Apparent Activation Energy of CO or CO_2 Hydrogenation*

The apparent activation energy was determined according to the Arrhenus equation,

$$r = k \cdot e^{-E_a/RT}$$

Where, E_a is the apparent activation energy; k is the product of the frequency factor of the rate constant, A_o, and the constant concentration maintained through out the experiment. The results for the total reaction and for each product formed from CO and CO_2 hydrogenation are shown in Tables 3 and 4. Here the partial pressure of CO or CO_2 was maintained at approximately 0.5 and CO_x/H_2 ratio was 1.

Generally, apparent activation energy data show good agreement with activity and selectivity trends implied by the data mentioned above. It can be seen that the total E_a of CO hydrogenation on cluster-derived catalysts are significantly lower than that on separate complex-derived catalysts. The E_a of oxygenate formation from CO on cluster-derived catalysts are lower than that of other catalysts. Similarly, for CO_2 hydrogenation, cluster-derived catalysts exhibit lower total Ea and significantly lower Ea of oxygenate formation compared with the other catalysts examined. The most surprising results are the negative Ea! Evidently, promotion by Mo of Rh for CO or CO_2 conversion and oxygenate formation is much more effective when the catalysts are made from Rh-Mo bimetallic clusters. Another interesting results from the study of apparent activation energies, which is not appeared in the Table 1, is the decline in E_a of CO hydrogenation on the cluster-derived catalysts with the reaction time during the initial 50 hours on stream. For example, total E_a of CO hydrogenation on $RhMo/SiO_2$ decreased from 127KJ/mol in the 3rd hour on stream to 88KJ/mol at the 30th hour and stabilized to about 73KJ/mol. The mononuclear complex-derived catalysts did not exhibit significant changes in total E_a with the reaction time. This decrease in E_a with time for the cluster-derived catalysts suggests that the nature and number of active sites on this catalyst are

transformed in the presence of the reactant gases at reaction conditions. All the E_a data included in the tables are reported when the reaction reached its stable activity.

5. *Reaction Orders with Respect to Partial Pressure of H_2 and CO or CO_2*

In order to obtain the kinetic information for CO or CO_2 hydrogenation related to the total reaction and each component formed, the reaction rates were measured while changing partial pressures of H_2 and CO or CO_2. Using the least-square regression method, the power law reaction orders were determined from the data and are listed in Tables 5 and 6.

It can be seen from Table 5 that reaction orders with respect to the partial pressure of H_2 are all positive for all components formed and the reaction orders with respect to CO are mostly negative for hydrocarbon and oxygenate formation in the CO hydrogenation reaction. Although reaction orders of oxygenate formation with respect to H_2 on the cluster-derived catalysts are slightly lower than that on the mononuclear complexes derived catalysts, the CO inhibition effect of oxygenate formation on the cluster-derived catalysts is significantly weaker than that on mononuclear complex-derived catalysts. The oxygenate formation rate order with respect to CO is even positive for $RhMo/SiO_2$. Therefore, superior oxygenate selectivity of the cluster-derived catalysts in CO hydrogenation may be explained as the result of weak inhibition of CO or even a promotion of CO to oxygenate formation. Generally, the trends for promotion effects with respect to the partial pressure of H_2 and inhibition effects with respect to the partial pressure of CO on the Rh-Mo bimetallic catalysts reported here are in agreement with the results of the silica-supported Rh, Rh-Fe, Rh-Li, or Rh-Mn catalysts reported by Burch and Petch[12c].

Similarly, reaction orders with respect to H_2 for all products formed are positive in the CO_2 hydrogenation reaction, with the exception of total reaction and CO formation on $Rh,Mo/Al_2O_3$, where the values are slightly negative. The reaction orders with

respect to CO_2 for all product formations are negative. The stronger H_2 promotion and weaker CO_2 inhibition for oxygenate formation on cluster-derived catalysts compared to that on the mononuclear complex-derived catalysts is in good agreement with the results described above.

6. *IR Evidence of Different Surface Features of the Catalysts*

Fourier Transform infrared (FTIR) spectra were recorded *in situ* for all catalysts after reduction at 350°C, absorption of CO at 50°C and evacuation at room temperature. The spectra are shown in Figures 5 and 6.

The FTIR spectroscopy study indicates that CO chemisorption on the cluster-derived catalysts has mainly gem-dicarbonyl features in contrast with the principally linear-CO coordination characteristics of the mononuclear complex-derived catalysts. This interpretation of the observed IR bands are mainly based on the summary of CO absorption on supported Rh catalysts by G. H. Olive and S. Olive in their extensive review[16]. According to the review, a doublet with component peaks at 2101 and 2031 cm^{-1} was assigned to symmetric and antisymmetric vibration of dicarbonyls on Rh^+ species, the broad band at 1855 to 1870 cm^{-1} and band at 2056 to 2070 cm^{-1} were assigned to bridging CO, $Rh_2(CO)$, and linear RhCO species on more "crystalline" island or rafts of Rh, respectively.

The carbonyl absorption characteristics of the IR spectra on the catalysts also show some variation with the oxide support used. On $RhMo/SiO_2$, strong gem-dicarbonyl absorption appeared at 2103 and 2033 cm^{-1}, broad weak-bridging absorption appeared at 1900cm^{-1} and almost no linear-CO absorption was observed. In contrast, on $RhMo/Al_2O_3$, there was distinct linear-CO absorption (2065 cm^{-1}) besides the similar gem-dicarbonyl (2096, 2026 cm^{-1}) and broad weak-bridging (1863 cm^{-1}) CO absorption. These differences in CO absorption may contribute to the different oxygenate distributions on the cluster-derived catalysts supported by different oxides. The differences in CO absorption between the mononuclear complex-derived catalysts and the

cluster-derived catalysts are evident in both the silica- and alumina-supported cases. Not only were there no gem-dicarbonyl bands on the mononuclear complexes-derived catalysts, but also the linear-CO peak positions are shifted from 2075 cm^{-1} to 2055, 2033 cm^{-1} for $Rh,Mo/SiO_2$, and from 2065 to 2076 cm^{-1} for $Rh,Mo/Al_2O_3$.

It has been reported[5-7] that the gem-dicarbonyl became the main species on the surface of supported rhodium catalysts only when the Mo/Rh ratio is high (>4). The gem-dicarbonyl feature was also thought to be a evidence of a high dispersion of rhodium[7]. However, strong gem-dicarbonyl absorptions were observed on the cluster-derived catalysts in this study, where the Mo/Rh ratio is only 1. After comparison with the IR spectra of mononuclear complex-derived catalysts with the same metal loading, it is evident that the gem-dicarbonyl feature of the cluster-derived catalysts is not a result of low metal loading in this work, though low Rh loading was found to give rise to gem-dicarbonyl on supported Rh catalysts[16]. Therefore, the gem-dicarbonyl feature of the CO absorption on the cluster-derived catalysts might imply a more effective electronic promotion by the molybdenum on rhodium. This more effective electronic promotion may be related to the strong Rh-Mo interaction in the precursor which may be a double bond as evidenced by its short bond length (2.588Å)[9]. The strong bimetallic interaction in the precursor might be maintained to some extent in the derived catalysts. This strong interaction between Rh and Mo could leave rhodium partially electropositive and allow molybdenum to stay in a lower oxidation state, i.e. electronic density could shift from Rh towards Mo during reduction and/or reaction. The special surface feature of the cluster-derived catalysts may correlate to the superior oxygenate selectivity in CO_x hydrogenation.

7. Effect of Phosphorus

So far, no direct data demonstrate the effect of the presence of phosphorus on the catalysts, but it seems clear that phosphorus could potentially inhibit the activity of Rh-Mo bimetallic catalysts for CO or CO_2 hydrogenation to some extent. Nevertheless, the cluster-derived catalysts indeed show higher activity and superior oxygenate selectivity compared with mononuclear complex-derived catalyst where both contain phosphorus. Phosphorus present on the surface, while often considered to be a inhibitor to metallic catalysts, may block some active sites on the surface for hydrocarbon formation and decrease hydrocarbon selectivity. Actually, the inhibitor could be a useful factor when it inhibits undesired side reactions, e.g. hydrocarbon formation, more than the desired reaction, e.g. oxygenate formation. The key factor here is that the inhibitor must selectively obstruct some of the catalytic sites. Modification of the cluster precursor would be the best choice for designing highly selective CO hydrogenation catalysts not only from the standpoint of specific structural features of metals in it, but also because this would allow the introduction of various kinds of ligands at specific positions on the metallic skeleton as potential selective inhibitors. The further development of the organometallic chemistry offers great opportunities and possibilities for approaching this goal.

Conclusions

Rh-Mo catalysts derived from the bimetallic cluster, $(PPh_3)_2RhMo(CO)(\mu\text{-}CO)_2Cp$, show higher activity and superior oxygenate-selectivity in CO and CO_2 hydrogenation reaction compared with catalysts derived from the mononuclear complexes, $RhH(CO)(PPh_3)_3$ and $[Mo(CO)_3(C_5H_5)]_2$. The propensity for oxygenate formation on the cluster-derived catalysts was also confirmed by derived data for apparent activation energies and reaction orders. Gem-dicarbonyl was the main CO-absorbed species on the cluster-derived catalysts, and this implied that rhodium exist as

+1 oxidation state. These IR results suggest that promotion of Rh by Mo might occur through a partial electron transfer from Rh to Mo.

References

1. A. Trunschke, H. Ewald, D. Gutschick, H. Miessner and M. Skupin, B. Walther, and H. C. Bottcher, *J.Mol.Catal* , **56**, 95(1989).
2. A. Trunschke, H. Ewaald, H. Miessner, A. Fukuoka, and M. Ichikawa, *Mater.Chem.and Phys.*, **29**, 503(1991).
3. A. Trunschke, H. C. Bottcher, A. Fukuoka, M. Ichikawa, H. Miessner, and H. C. Bottcher, *Catal. Lett.*, **8**, 221(1991).
4. R. Lamber , N. I. Jaeger, A. Trunschke, and H. Miessner, *Catal. Lett.*, **11**, 1(1991).
5. B. J. Kip, E. G. F. Hermans, J. H. M. C. Van Wolput, N. M. A. Hermans, J. Van Grondelle and R. Prins, *Appl. Catal.* **35**, 109(1987).
6. E. C. DeCanio and D. A. Storm, *J. Catal.* **132**, 375(1991).
7. M. D. Wardinsky and W. C. Hecker, *J.Phys.Chem.*, **92**, 2602(1988).
8. A. Trunschke, H. Ewald and H. Miessner et al., *J.Mol.Catal.*, **74**, 365(1992).
9. L. Carlton, W. E. Lindsell, K. J. McCullough and P. N. Preston, *J.Chem.Soc. Dalton Trans.*, 1693(1984).
10. H. C. Foley, A. J. Hong, J. S. Brinen, L. F. Allard, and A. J. Garratt-Reed, *Appl. Catal.*, **61**, 351(1990).
11. C. Sudhakar, N. A. Bhore, K. B. Bischoff, W. H. Manogue, and G. A. Mills, *Catalysis 1987*, J. W. Ward Ed., Elsevier Sc. Pub., Amsterdam, 115(1988)

12. R. Burch and M. I. Petch, (a) *Appl. Catal.* A: **88**, 39(1992). (b) ibid, **88**, 61(1992). (c) **88**, 77(1992).

13. F. Fischer and H. Tropsch, *Chem. Ber.*, **59**, 830(1926)

14. F. Fischer and H. Tropsch, *Brennst. Chem.*, **7**, 97(1926)

15. A. Behr *Carbon Dioxide Activation by Metal Complexes* p15. VCH Verlagsgesellschaft (Germany) 1988.

16. G. Henrici-Olive and S. Olive, *The Chemistry of the catalyzed Hydrogenation of Carbon Monoxide* Page 40. Springer-verlag 1984.

Table 1. CO_2-free Seclectivity of Rh-Mo Bimetallic Catalysts for CO Hydrogenation

Catalysts[a,b]	H_2/CO	T°C	P(MPa)	CxHy	MeOH	Me_2O	EtOH	ΣOxy.	r[c]
RhMo/SiO2	2	300	2.0	21.6	73.5	0.3	4.4	78.2	10.0
Rh,Mo/SiO2	2	300	2.0	48.0	41.5	/	10.5	52.0	9.0
RhMo/Al2O3	2	250	1.87	24.8	17.8	44.9	12.4	75.1	64.0
Rh,Mo/Al2O3	2	300	2.0	37.4	19.9	42.7	/	62.5	2.4

a. RhMo and Rh,Mo represent catalysts derived from $RhMo(CO)_3Cp(PPh_3)_2$ and the mixture of $RhH(CO)(PPh_3)_3$ and $[Mo(CO)_3Cp]_2$, respectively.

b. Calculated Rh loading is 0.5%wt and Rh/Mo mole ratio is 1 for all catalysts.

c. Total reaction rate in the unit of 10^{-6}xMol CO/gRh/Sec.

Table 2. CO-free Selectivity of Rh-Mo Bimetallic Catalysts for CO_2 Hydrogenation

Catalysts[a]	H2/CO2	T°C	P(MPa)	CxHy	MeOH	Me2O	EtOH	ΣOxy.	r[b]
RhMo/SiO2	1	300	2.0	36.3	61.9	/	1.9	63.8	1.78
Rh,Mo/SiO2	1	350	2.0	59.5	39.5	/	1.0	40.5	2.50
RhMo/Al2O3	1	300	2.0	43.4	44.1	8.7	3.9	56.6	2.00
Rh,Mo/Al2O3	1	350	2.0	55.8	43.0	1.2	/	44.2	1.92

a. The catalysts are same with table 1.

b. Total reaction rate in the unit of 10^{-6}xMol CO_2/gRh/Sec.

Table 3. Apparent Activation Energy of $CO+H_2$ on Bimetallic Catalysts (KJ/mol)

	$RhMo/SiO_2$	$Rh,Mo/SiO_2$	$RhMo/Al_2O_3$	$Rh,Mo/Al_2O_3$
Total reaction	73	93	85	102
CH_4	92	104	129	129
C_2H_6	100	105	152	122
C_3H_8	88	100	133	113
C_4H_{10}		108	123	83
MeOMe			63	67
MeOH	60	66	78	79
EtOH	56	71	69	

Table 4. Apparent Activation Energy of CO_2+H_2 on Bimetallic Catalysts (KJ/mol)

	$RhMo/SiO_2$	$Rh,Mo/SiO_2$	$RhMo/Al_2O_3$	$Rh,Mo/Al_2O_3$
Total reaction	54	68	64	67
CO	54	68	66	67
CH_4	90	89	105	93
C_2H_6	92	111	92	84
C_3H_8	97	120	96	85
MeOMe	-17		-27	-31
MeOH	-24	19	-4.2	19
EtOH			-32	

Table 5. CO Hydrogenation Reaction Orders

Products	$RhMo/SiO_2$	$Rh,Mo/SiO_2$	$RhMo/Al_2O_3$	$Rh,Mo/Al_2O_3$
Reaction orders with respect to H_2				
Total	0.54	0.73	0.08	0.06
CO_2	0.49	0.84	0.01	0.33
CH_4	0.75	0.97	0.76	0.81
C_2H_6	0.47	0.55	0.73	0.56
C_3H_8	0.42	0.53	0.61	0.09
C_4H_{10}	0.26		0.08	
MeOMe			0.96	1.36
MeOH	0.73	1.15	0.69	0.76
EtOH	0.82	0.77	0.50	
Reaction orders with respect to CO				
Total	0.68	0.06	-0.11	-0.35
CO_2	0.83	0.69	0.08	0.59
CH_4	-0.48	-0.29	-0.76	-0.25
C_2H_6	-0.33	-0.17	-0.27	-0.14
C_3H_8	0.07	0.03	0.36	0.48
C_4H_{10}	-0.45		0.49	
MeOMe			-0.84	-0.76
MeOH	0.49	-0.35	-0.24	-1.54
EtOH	0.37	-0.55	-0.94	

Table 6. CO_2 Hydrogenation Reaction Orders

Products	$RhMo/SiO_2$	$Rh,Mo/SiO_2$	$RhMo/Al_2O_3$	$Rh,Mo/Al_2O_3$
Reaction orders with respect to H_2				
Total	0.46	0.3	0.29	-0.31
CO	0.28	0.3	0.29	-0.40
CH_4	0.49	0.55	0.79	0.66
C_2H_6	0.54	0.73	0.21	0.14
C_3H_8	0.43	1.30	0.45	0.62
MeOMe			0.89	1.35
MeOH	0.35	1.42	0.35	1.23
EtOH	-0.47		0.36	
Reaction orders with respect to CO_2				
Total	-0.06	-0.22	-0.13	-0.61
CO	-0.21	-0.22	-0.11	-0.68
CH_4	-0.85	-1.30	-0.47	-0.80
C_2H_6	-0.34	-1.50	-0.55	-1.42
C_3H_8	-0.19	-1.76	0.25	-0.81
MeOMe			-1.84	-2.8
MeOH	-1.27	-1.67	-1.15	-0.81
EtOH	-1.74		-0.42	

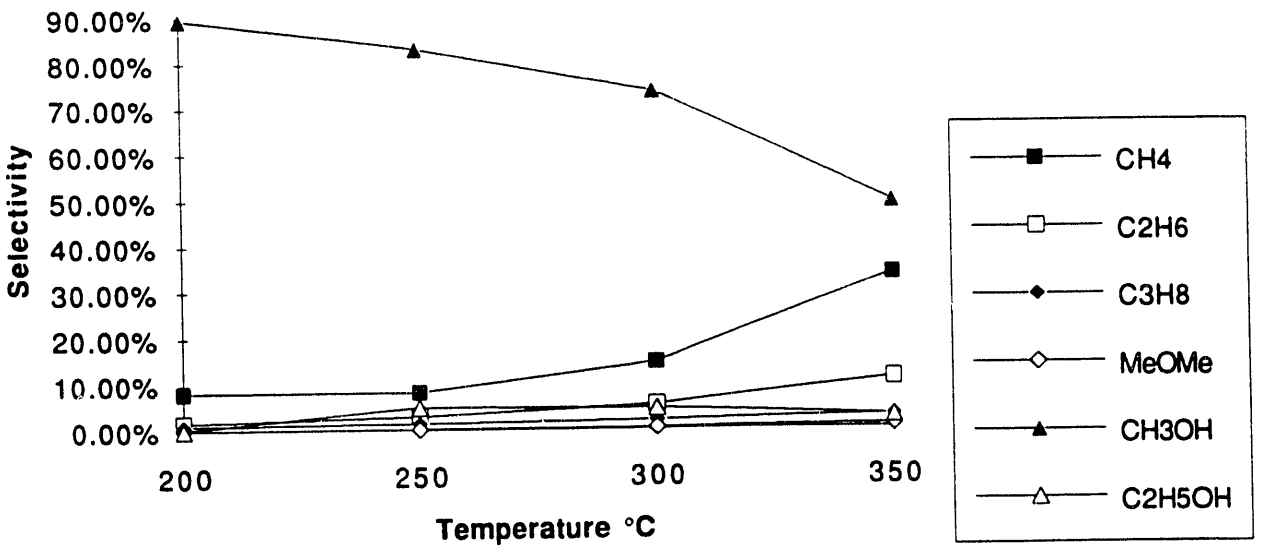

Figure 1. Temperature dependences of selectivities on RhMo/SiO2 (300psi, CO/H2=1/2)

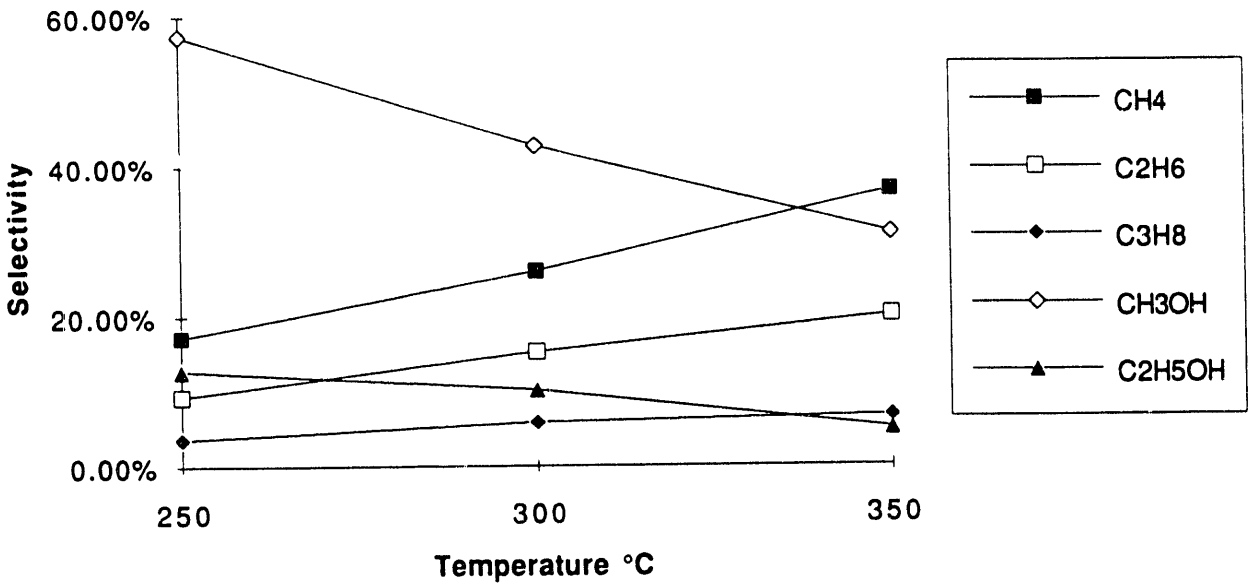

Figure 2. Temp. dependences of selectivities Rh,Mo/Al2O3, 300psi, CO/H2=1/2.

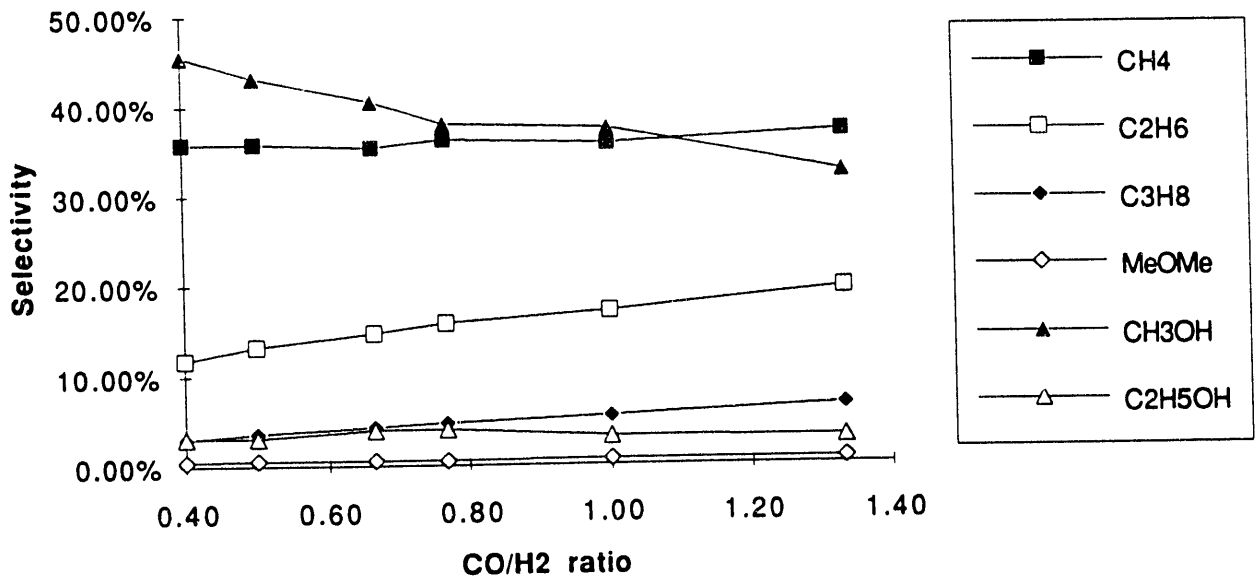

Figure 3. Effect of CO/H2 ratio on selectivity (RhMo/SiO2, 350°C, 300psi)

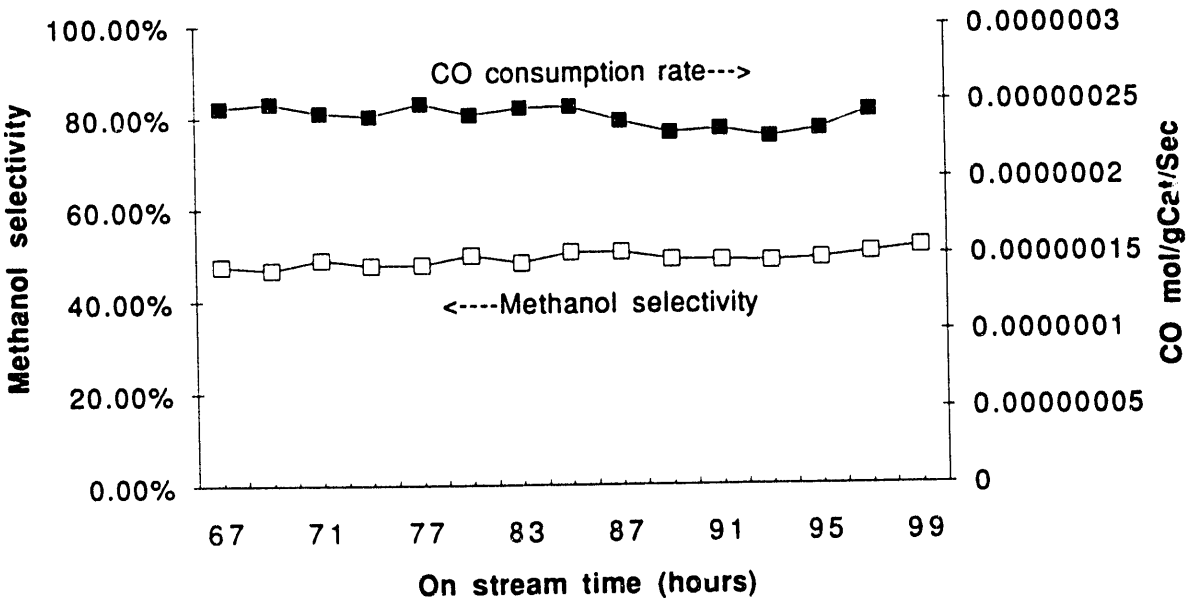

Figure 4. Stability of RhMo/SiO2(350°C, 300psi, CO/H2=1/2)

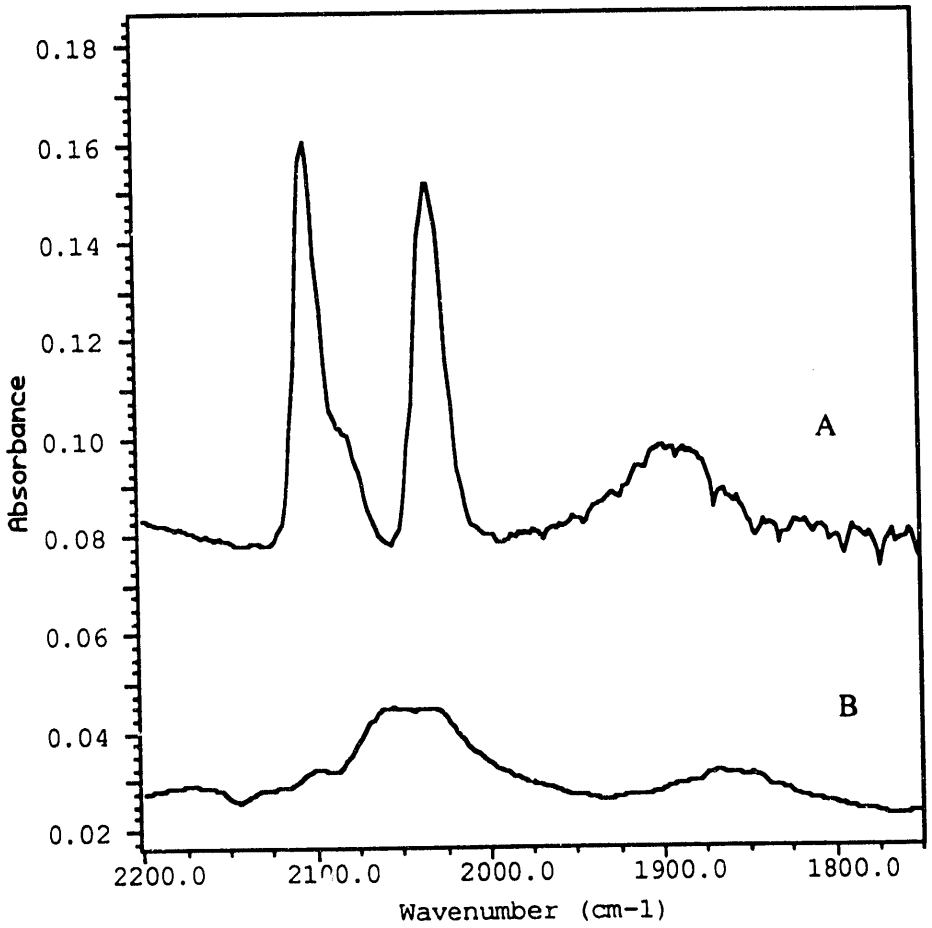

Fig. 5 A: CO-absorbed RhMo/SiO2 evacuated at RT
B: CO-absorbed Rh,Mo/SiO2 evacuated at RT

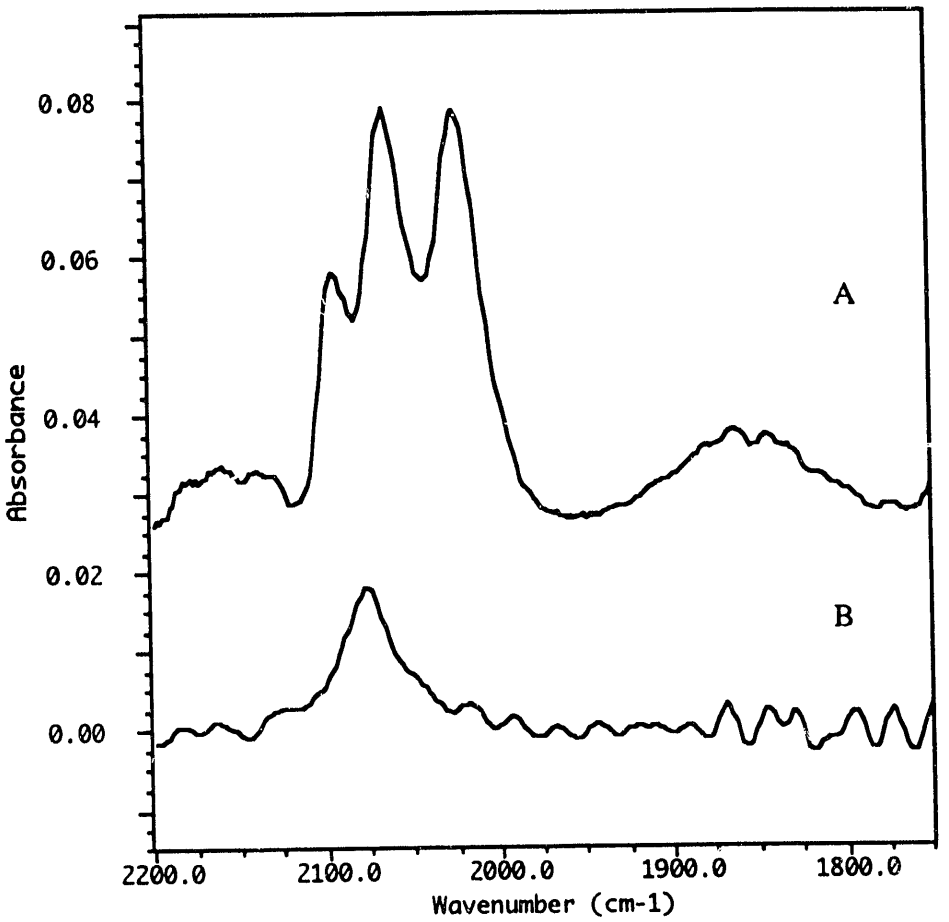

Fig. 6 A: CO-absorbed RhMo/Al2O3 evacuated at RT
B: CO-absorbed Rh,Mo/Al2O3 evacuated at RT.

END

DATE
FILMED
4/1/93